Generalized theory of the total fracture surface energy for glassy organic polymers

R. P. Kusy and M. J. Katz
Dental Research Center, University of North Carolina at Chapel Hill, Chapel Hill, North Carolina 27514, USA
(Received 4 November 1977; revised 9 March 1978)

A model is presented that describes the molecular weight dependence of the total fracture surface energy (γ) on glassy organic polymers from monomeric values ($\gamma \approx 30$ erg/cm^2) to viscosity-average molecular weights ($\bar{M}_v$) greater than 10^6 [$\gamma = 1.4 \times 10^5$ erg/cm^2 for poly(methyl methacrylate) (PMMA); $\gamma \approx 10^6$ erg/cm^2 for polystyrene (PS)]. The empirical expressions for PMMA and PS combine the energy contributions from the free surface, the cleavage of covalent bonds, and the viscous flow of molecules by assuming a random molecular weight distribution, the critical chain length necessary to permit viscous flow (x), and the entanglement molecular weight (ϵ). From cleavage and notched tensile bar tests prepared either by solution polymerization or by radiation degradation of commercial PMMA, the overall structure–property relationship is described.

INTRODUCTION

Fox and Zisman characterized the specific surface free energy (γ_0) of liquids (such as monomers) and 'soft organic solids' (such as waxes, solid organic polymers, and most solid organic compounds) as being < 100 erg/cm^2 [1,2]. Experiments have shown, however, that high polymers fractured under a variety of conditions exhibit values for γ in excess of the theoretical value necessary to cleave a monolayer of covalent bonds, i.e. $\gamma \approx 10^5$–10^6 *versus* ≈ 500 erg/cm^2, respectively[3,4]. Since several processes may contribute to the total surface work, polymers may yield results over a broad range of γ, dependent principally on the molecular weight.

In the oligomeric region, several investigators have studied the surface tension (γ_0) of polymeric liquids[2,5–13]. These have included the homologous series of the n-alkanes (C_5–C_{18}) and the n-alkenes (C_6–C_{16})[8], the polyorganosiloxanes (dimer to heptadecamer)[6], the poly(ethylene glycols) (including the heptamer)[5,7], and the perfluoroalkanes[10]. In addition, a series of polymers of nylon (6 to 11 and 6,6 to 10,10)[2] has been studied by contact angle measurements and in the case of polystyrene ($\bar{M}_n = 10^3$–10^4)[11] at elevated temperatures by the pendant drop method. From these efforts two nearly equivalent expressions have been used to describe the dependence of surface tension of polymer liquids on the molecular weight:

$$\gamma_0 = \gamma_\infty - (k_e/\bar{M}_n{}^{2/3}) \qquad \text{(refs 10 and 11)} \qquad (1a)$$

or

$$\gamma_0^{-1/4} = \gamma_\infty^{-1/4} + (k_s/\bar{M}_n) \quad \text{(ref 13)} \qquad (1b)$$

From these functional relationships, γ_0 varies from 15–45 erg/cm^2 for all series aforementioned. While γ_0 is a negligible contribution to γ for all the lowest molecular weights, the importance of γ_0 to the better understanding of wettability and adhesion cannot be overemphasized.

In the high molecular weight region, the total fracture surface energy (γ) has been determined, principally on commerical grade materials[3,4,14–30]. Variables that have been considered include the dependence of γ on molecular orientation[24], temperature[16,20,23], sample geometry[21,25,27,28], degree of crosslinking[20,24], strain rate (i.e. the crack velocity)[16,25,26], and molecular weight[16,22,27–30]. Of these, molecular weight has shown changes far in excess of one order of magnitude. For example, in PMMA[28] the most reliable γ measurements conducted at low crack velocities ($\dot{a} < 0.1$ cm/sec at 20°C) have ranged from 750 to 1.1×10^5 erg/cm^2 for $2 \times 10^4 < \bar{M}_v < 1.2 \times 10^6$; while for PS[16–19,21,23,29], values have ranged from 175 to $\sim 5 \times 10^5$ erg/cm^2 for $3.5 \times 10^3 < \bar{M}_v < 5 \times 10^5$. Below $\bar{M}_v = 2 \times 10^4$ (PMMA) a large deficiency exists in the current knowledge of the relationship of γ to M, due partly to the extreme difficulty of fabricating and physically testing such brittle materials[20,30]. The present objective is to determine values of γ for PMMA prepared by solution polymerization and by the systematic radiolysis of commercial polymer down to $\bar{M}_n \sim 1.6 \times 10^3$ using cleavage bar or notched tensile bar techniques. With this PMMA data and the PS data abstracted from the literature, the proposed theory for the fracture surface energy of glassy organic polymers is assessed.

NOTATION

The following nomenclature is used throughout the text. Standard notation is abandoned only in cases in which duplicity between disciplines has occurred.

a	Beam constant
$\dot{a}$	Fracture velocity
A,B	Property constants
c	Natural flaw length
d_1,d_2	Depths of saw cuts
E	Young's modulus

0032–3861/78/111345–13$02.00

f	Applied load
k	Exponent in the Schulz distribution equation
k_e, k_s	Surface tension constants
K, α	Viscosity constants
L	Liquid state
l	Propagated crack length
M_0	Molecular weight of a mer
$\bar{M}_n$	Number-average molecular weight
$\bar{M}_v$	Viscosity-average molecular weight
$\bar{M}_w$	Weight-average molecular weight
n	Beam exponent
P	Property
r	The rth mer
s	Solid state
s_1, s_2	Girths of saws
t	Specimen thickness
T_g	Glass transition temperature
U_0	Bond breaking energy
w	Specimen width
ω	Crack width
W	Weight fraction
x	Critical degree of polymerization necessary for plastic deformation
$\bar{x}_n$	Number-average degree of polymerization
x_t	Degree of polymerization below which non-solvent has solvent power
γ	Total fracture surface energy
γ_0	Surface tension component of total fracture surface energy
γ_1	Covalent bond fracture energy component of total fracture surface energy
γ_2	Plastic deformation fracture energy component of total fracture surface energy
γ_c	Plastic deformation fracture energy of infinite molecular weight polymer
γ_ϵ	Fracture surface energy at the entanglement degree of polymerization
γ_∞	Surface tension of infinite molecular weight polymer
δ	Deflection of one cantilever beam
δ'	Total apparatus deflection
Δ	Instron machine deflection
ϵ	Entanglement degree of polymerization
η	Kinematic viscosity
υ	Poisson's ratio
σ_f	Tensile strength at failure

MODEL

Historical development

The earliest attempt to generate any relationship between γ and $\bar{M}_n$ (Berry, 1964)[27] utilized the form:

$$P = A - (B/\bar{M}_n), \tag{2}$$

in which a property (P) and $\bar{M}_n$ were related by two constants over the experimental range $9.8 \times 10^4 < \bar{M}_v < 6.0 \times 10^6$. Using the cleavage technique on PMMA test bars, equation (3) resulted:

$$\gamma = 1.55 \times 10^5 - (3.9 \times 10^9/\bar{M}_v) \tag{3}$$

As later work has shown[28], this form was appropriate for $\bar{M}_v \gtrsim 10^5$, below which the functional relationship assumed a concave upward appearance (ref 4 for PMMA; ref 29 for PS).

Recently, a theoretical dependence of fracture surface energy on molecular weight in PMMA was derived on the assumption that only molecules exceeding a critical degree of polymerization (x) could contribute to the work of plastic deformation[27]. The form of the expression assumed that the viscous flow term (γ_2) and the energy required to rupture a monolayer of covalent bonds (γ_1) equalled the total fracture surface energy, or:

$$\gamma = \gamma_1 + \gamma_2 \tag{4}$$

With the substitution and integration of the most probable molecular weight distribution for PMMA ($k = 1$), equation (4) became:

$$\gamma = \gamma_1 + \gamma_c(e^{-x/\bar{x}_n})\,[1 + (x/\bar{x}_n)] \tag{5}$$

in which $\bar{x}_n$ was the number-average degree of polymerization and γ_c was a constant-energy term $\approx \gamma$ as $\lim \bar{x}_n \to \infty$. (Note that γ_c used here is not to be confused with the critical surface tension of wetting). *Figure 1* compares equation (5) with previous notched tensile bar data.

While, in general, equation (5) is valid for $\bar{x}_n \gtrsim 150$ ($\bar{M}_v \gtrsim 3 \times 10^4$ for PMMA) and the precise molecular weight distribution is of secondary importance, two immediate shortcomings of this model are seen. Firstly, the γ_c was provisionally assumed to equal the notched tensile bar value of 3.5×10^5 erg/cm^2. The selection of that value was properly chosen at that time to assess the general validity of the functional relationship with respect to the available experimental data. However, that data reflected the crack velocity ($\dot{a}$) sensitivity shown to exist in polymers undergoing viscous flow[26]. According to Kambour and Barker[31], such complications could be avoided if negligible temperature rises were ensured by fracturing at $\dot{a} < 1$ cm/sec, in good agreement with later experimental measurements by Williams, Radon and Turner[32] and Marshall, Culver and Williams[25]. Such an account of $\dot{a}$ is made in the cleavage bar measurements of Berry[22] and of Kusy and Katz[28], in which $\gamma_c \approx 1.4 \times 10^5$ erg/cm^2 (*Figure 2*). Note that a satisfactory fit between theory and experiment is achieved when $x \approx 900$. The value $\bar{M}_n \sim 90\,000$ agrees qualitatively with specific morphological changes observed in PMMA – the creation of vast zones of parabolic markings (e.g. in the mist region) and the proliferation of interference colours (crazing) – both indicative of significant plastic deformation[33].

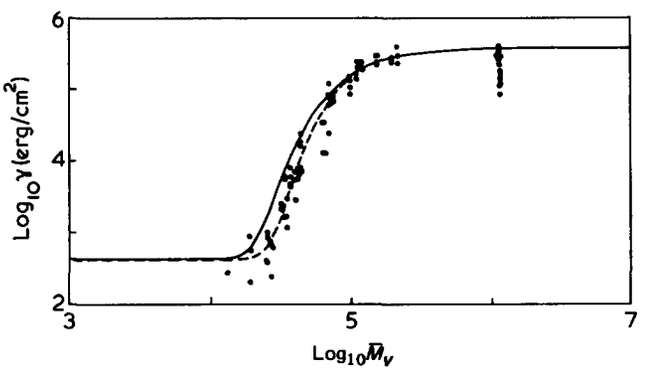

Figure 1 Comparison of earlier model (equation 5) with previous PMMA notched tensile bar data (see *Figure 7* of ref 27) where x = 1000. ——, $k = 1$; – – – –, $k = 2$

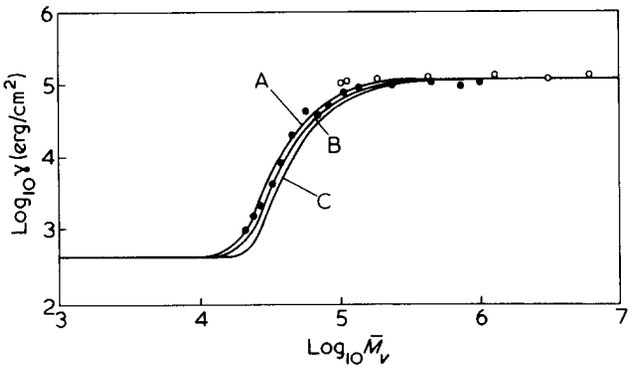

Figure 2 Comparison of earlier model (equation 5) with previous PMMA parallel cleavage bar data in which $k = 1$. ○, Berry[22]; ●, Kusy and Katz (data reported as mean of *Tables 2* and *3* of ref 28). A, x = 800; B, 900; C, 1000

Secondly, below the molecular weight at which viscous flow mechanisms occur, γ was considered to be constant at ≈ 500 erg/cm^2 (*Figure 2*). While it is reasonable that $\gamma \approx 500$ erg/cm^2 for molecular weights just less than those at which viscous flow processes are operative, the constancy of the term is clearly an oversimplification; γ must ultimately decrease to ≈ 30 erg/cm^2, the monomeric surface free energy. The above two observations, the critical degree of polymerization necessary for viscous flow to occur (x), and the role of entanglement molecular weight in the deformation process (ϵ) are necessary to define a theory of γ for glassy polymers.

Generalized theory

Dependent upon parameters such as test temperature, pressure, and strain rate, the fracture surface energy of a material may be composed of up to three parts: the energy of deformation (γ_2), the energy of breaking (γ_1), and the cohesive surface free energy (γ_0).

$$\gamma = \gamma_0 + \gamma_1 + \gamma_2 \tag{6}$$

Here, the principle of superposition is used because of the consecutive nature of the failure process in which deformation precedes the breaking of covalent bonds and the parting of surfaces (see ref 34). While in polymers the number and extent of processes operative is also dependent on the degree of crosslinking, extent of branching, percent crystallinity, and their respective distributions, molecular weight effects predominate in a simple glassy organic polymer. As a minimum requirement, analysis of γ is dependent on a thorough understanding of the predominant component within a particular molecular weight range.

For the homologous series of a glassy organic polymer, reliable knowledge of three molecular weights or molecular ranges is essential: the transition number-average degree of polymerization from liquid to solid state behaviour $(\bar{x}_n)_{L\to s}$, the entanglement degree of polymerization (ϵ), and the critical degree of polymerization for viscous flow (x). Initially, the monomer exhibits only the surface tension that is characteristic of an organic liquid (γ_0), which increases slightly as the free volume or density changes (*Figure 3*). At ambient temperatures, molecules slide past one another; there is no need for covalent bond rupture. However, at some point (usually $\bar{x}_n = 10$–30), viscosity increases sufficiently so that the material properties are very sensitive to strain rate changes. Near this junction, i.e. when $\bar{x}_n = (\bar{x}_n)_{L\to s}$, where $T_g \approx$ ambient temperature, covalent bonds may begin to break (γ_1), although the magnitude of the surface tension term predominates. Soon, the energy required to break the covalent bonds dominates the total fracture surface energy until roughly one third of the covalent bonds rupture at failure. At this value of ϵ, the surface tension term has long since saturated to a constant value and viscous flow processes (γ_2) begin. Concurrent with this viscous flow, more covalent bonds break since more molecules become aligned in the direction of principal stress. Moreover, even before crazing can be identified by brightly coloured features, the fracture energy resulting from viscous flow is dominant. As more and more molecules exceed the critical number of repeat units for viscous flow (x), crazing increases the energy absorbing capabilities about 1000 fold over the classical organic solid.

Referring again to equation (6), γ may be expressed as follows. For $\bar{x}_n \leq (\bar{x}_n)_{L\to s}$:

$$\gamma = \gamma_0 \tag{7}$$

$$= \gamma_\infty - \frac{k_e}{(M_0\bar{x}_n)^{2/3}} \tag{7a}$$

or

$$= \left(\frac{1}{\gamma_\infty{}^{1/4}} + \frac{k_s}{M_0\bar{x}_n}\right)^{-4} \tag{7b}$$

For $(\bar{x}_n)_{L\to s} \leq \bar{x}_n \leq \epsilon$:

$$\gamma = \gamma_0 + \gamma_1 \tag{8}$$

where γ_0 equals equations (7a) or (7b), and

$$\gamma_1 = \left(\frac{\gamma_\epsilon}{\epsilon - (\bar{x}_n)_{L\to s}}\right)[\bar{x}_n - (\bar{x}_n)_{L\to s}] \tag{8a}$$

For $\bar{x}_n \geq \epsilon$:

$$\gamma = \gamma_0 + \gamma_1 + \gamma_2 \tag{9}$$

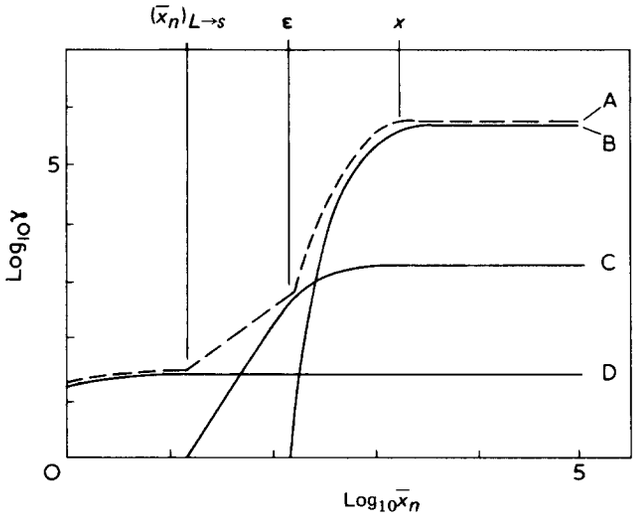

Figure 3 Schematic representation of the contributions to the total fracture surface energy (γ) as a function of the number-average degree of polymerization. A, γ; B, γ_2; C, γ_1 and D, γ_0

Table 1 Constants used for the determination of the total fracture surface energy of poly(methyl methacrylate) ($M_0 = 100$)

Term	Assigned value	Data source
γ_∞	42.4 erg/cm^2	Essentially the extrapolation to room temperature from molten state ($\bar{M}_v = 3000$)[39–41]
$k_e; k_s$	290.8; 3.937	Constants based on calculated γ of monomer (28.91 erg/cm^2 as determined from Parachor[42–44]) and γ_∞
γ_ϵ	480 erg/cm^2	Solution based on the rupture of 1/3 of the molecules in a cleavage plane ($\gamma_\epsilon = 450$ erg/cm^2, ref 3). The bond energy (U_0) was taken as 55 kcal/mol[45,46]
ϵ	80	Preferred value based on a group of data which range from $\bar{x}_n = 37$–106 (refs 47–49)
$(\bar{x}_n)_{L\to s}$	10	Assumed from $(\bar{M}_v)_{L\to s} \sim 2000$ and $(\bar{M}_v/\bar{M}_n) \sim 2$
x	900	Estimated from cleavage bar measurements[28] and fracture morphology[33], and confirmed by earlier theoretical treatment of γ_2[27]
γ_c	140 000 erg/cm^2	Preferred solution based on measurements conducted at slow à[22,28]

where

$$\gamma_0 = \gamma_\infty \tag{9a}$$

$$\gamma_1 = \gamma_\epsilon + 2\gamma_\epsilon \left[1 - \int_0^x W(r)\,dr\right] \tag{9b}$$

$$\gamma_2 = \gamma_c \left[1 - \int_0^x W(r)\,dr\right] \tag{9c}$$

For $\bar{x}_n \leqslant \epsilon$, γ_0 equals either the empirical surface tension expression of Gaines and LeGrand[10] or the derived expression of Wu[13]. In the range $(\bar{x}_n)_{L\to s} \leqslant \bar{x}_n \leqslant \epsilon$, however, γ_1 requires some speculation. On the premise that the molecules are sufficiently long enough by $(\bar{x}_n)_{L\to s}$ so that individual chain length and not chain end effects are the controlling factor, a linear relationship is assumed where each additional mer contributes an equal increment to γ_1. This is analogous to the functional relationship that exists between η and $\bar{M}_v$ over the same range[35]. Since entanglements are negligible for $\bar{x}_n < \epsilon$, $\gamma_2 = 0$.

For $\bar{x}_n > \epsilon$, γ_0 equals the surface tension of an infinite molecular weight polymer. Wu has reported that this is a valid approximation for $\bar{M}_n > 3000$, γ differing from γ_∞ by less than 1 erg/cm^2 [13]. [Moreover, for poly(vinyl acetate) having a $\bar{M}_w$ = 11 000–120 000, no significant change in γ was noted[36].] The last two terms, γ_1 and γ_2, are the most sensitive to x and molecular weight distribution. γ_1 approaches $3\gamma_\epsilon$ as $\lim \bar{x}_n \to \infty$; this corresponds to the cleavage of covalent bonds in the bulk of the polymer molecules that were transformed into bundles of fibrils within the crazed region. Further, when $\bar{x}_n \gg x$, the maximum extent of the crazed region is realized, i.e. $\gamma \approx \gamma_2 \approx \gamma_c$. While important to the overall interpretation of the failure phenomena, the second term of γ_1 (equation 9b) is effectively zero for $x \gg \bar{x}_n \gtrsim \epsilon$ and negligible when compared with γ_2 for $\bar{x}_n \gtrsim x$. To simplify future computations, $2\gamma_\epsilon$ is implicit in the value of γ_c chosen for γ_2 (equation 9c).

Application

Poly(methyl methacrylate). Equations (11)–(13) are obtained by assuming a Schulz-type molecular weight distribution:

$$W(r) = \left(\frac{k}{\bar{x}_n}\right)^{k+1} \left(\frac{r^k}{k!}\right) \exp\left(\frac{-kr}{x_n}\right); 1 \leqslant k \leqslant 2 \tag{10}$$

where $W(r)$ is the weight fraction of the rth mers for a given $\bar{x}_n$ [37]. For the most probable distribution ($k = 1$)[38], subsequent integration and substitution yields:

For $\bar{x}_n \leqslant 10$:

$$\gamma = 42.4 - (13.5/\bar{x}_n^{2/3})$$

or

$$\gamma = [0.3919 + (0.03937/\bar{x}_n)]^{-4} \tag{11}$$

For $10 \leqslant \bar{x}_n \leqslant 80$:

$$\gamma = 42.4 - (13.5/\bar{x}_n^{2/3}) + 6.86\,(\bar{x}_n - 10)$$

or

$$\gamma = [0.3919 + (0.03937/\bar{x}_n)]^{-4} + 6.86(\bar{x}_n - 10) \tag{12}$$

For $\bar{x}_n \geqslant 80$:

$$\gamma = 522 + 1.4 \times 10^5 (e^{-900/\bar{x}_n})\,[1 + (900/\bar{x}_n)] \tag{13}$$

Table 1 summarizes the constants used in obtaining these equations. Indeed, when radiation is used to degrade the acrylic, experimental materials result which fit the most probable molecular weight distribution[38].

Polystyrene. Equations (14)–(16) are obtained by substitution of the values summarized in *Table 2*, assuming the same Schulz-type molecular weight distribution.

For $\bar{x}_n \leqslant 15$:

$$\gamma = 40.7 - (10.7/\bar{x}_n^{2/3})$$

or

$$\gamma = [0.3959 + (0.03134/\bar{x}_n)]^{-4} \tag{14}$$

For $15 \leqslant \bar{x}_n \leqslant 340$:

$$\gamma = 40.7 - (10.7/\bar{x}_n^{2/3}) + 1.34\,(\bar{x}_n - 15)$$

or

$$\gamma = [0.3959 + (0.03134/\bar{x}_n)]^{-4} + 1.34\,(\bar{x}_n - 15) \tag{15}$$

For $\bar{x}_n \geqslant 340$:

$$\gamma = 476 + 10^6(e^{-4500/\bar{x}_n})\,[1 + (4500/\bar{x}_n)] \tag{16}$$

Table 2 Constants used for the determination of the total fracture surface energy of polystyrene (M_0 = 104)

Term	Assigned value	Data source
γ_∞	40.7 erg/cm^2	Extrapolation to room temperature from molten state ($\bar{M}_v$ = 44 000)[39]
k_e; k_s	236.6; 3.259	Constants based on calculated γ of monomer (30.01 erg/cm^2 as determined from Parachor[42–44]) and γ_∞
γ_ϵ	435 erg/cm^2	Solution based on the rupture of 1/3 of the molecules in a cleavage plane (γ_ϵ = 450 erg/cm^2, ref 23). The bond energy (U_0) was taken as 54 kcal/mole[45,46,50]
ϵ	340	A typical literature value which range from $\bar{x}_n$ = 300–385[47,48]
$(\bar{x}_n)_{L\rightarrow s}$	15	Assumed value
x	4500	Estimate based on the comparative fracture morphology (i.e. craze thickness ratio) of polystyrene *versus* poly(methyl methacrylate)[51]
γ_c	1 000 000 erg/cm^2	Representative literature value which range from γ = 500 000–2 000 000 erg/cm^2 (refs 16–19, 21, 23)

Table 3 Schedule of cleavage test specimens prepared

Specimen no	Geometry (in)				Annealed[b]	Precracked[c]	Irradiated[d] dose profile (Mrad)
	Width (nominal)	Height	Length	Slot type[a]			
1	1/2	1	10	–	–	–	252
2	1/2	1	10	C	–	–	108
3	1/2	1	10	A	–	A	158 → 105
4	1/4	1	10	D	–	–	105
5	1/2	1	10	B	–	–	105
6	1/4	1	10	D	–	–	105
7	1/4	1	10	D	–	–	108
8	1/2	1	10	B	+	–	112 → 69
9	1/4	1	10	D	+	–	67 → 38
10	1/2	1	10	A	+	–	76
11	1/2	1	10	B	+	–	76
12	1/2	1	10	B	+	A	76 → 52
13	1/2	1	10	B	+	B	76
14	1/2	1	10	C	+	B	76
15	1/4	1	10	D	+	–	76
16	1/2	1	10	A	+	B	79
17	1/2	1	10	B	+	B	79
18	1/2	1	10	B	+	B	79
19	1/4	1	10	D	+	B	79
20	1/2	0.875	9.56	C	+	B	137
21	1/2	1	10	C	+	B	79

[a] Slots machined as follows (see *Figure 4a*, lower):

Type	Total % material removed	d_1 (for s_1 = 0.008 in)	d_2 (for s_2 = 0.006 in)
A	50	0.065	0.050
B	67	0.10	0.051
C	75	0.14	0.031
D	50	0.00	0.063

[b] +, for 24 h at 70°C; –, not annealed

[c] B, before irradiation; A, after irradiation; –, not precracked

[d] Constant dose profile of ^{137}Cs source to ±2%. For variable dose profile superimposed on a constant dose profile the first value corresponds to maximum dose at 10 in. mark; second value corresponds to minimum dose at 10 in. mark (see *Figure 5*)

EXPERIMENTAL

Preparation of cleavage bar test specimens

Specimens were machined from commercially available poly(methyl methacrylate) sheet, Plexiglas G (M_v = 1.1 × 10^6, Rohm and Haas Co., Philadelphia, Pa.) (see *Table 3* and *Figure 4a*).

Using gamma radiation the molecular chain length of these cleavage bars was reduced in a ^{137}Cs source at a dose rate of 0.2 Mrad/h. This lower dose rate alleviated the likelihood of immediate specimen failure due to spontaneous gas evolution[28]. Although a variable dose profile would result under normal circumstances (*Figure 5*, position I and corresponding portion of full line), most of the bars were periodically rotated 180° and repositioned in the source so that a constant dose profile was achieved (*Figure 5*, position II and corresponding portion of full line). This is graphically shown in the present case by transposing the % dose data obtained in position II in terms of the bar geometry of position I (broken line). When summed, the net dose rate equalled 0.1 Mrad/h.

Since there is an inherent tendency for the relative percent error of physical measurements to increase as a material becomes more brittle, several steps were taken to optimize specimen preparation. For example, the side slots were machined by using saws with the narrowest girth compatible with the depth requirements (*Figure 4a*, lower). In many cases, two different girths (s_1, s_2) were used to minimize the material loss, and hence the measurement error. To reduce the number of excursions from the slotted plane, the slot depths (d_1, d_2) were often 2/3 to 3/4 of the total bar width. To increase the data base, fiducial marks were made at

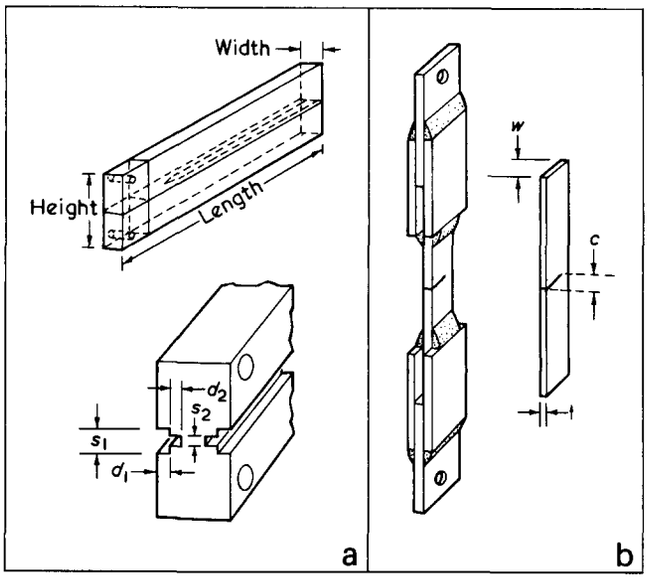

Figure 4 Illustration of the two types of fracture toughness specimens prepared: (a) parallel cleavage bars; (b) single edge notched tensile bars

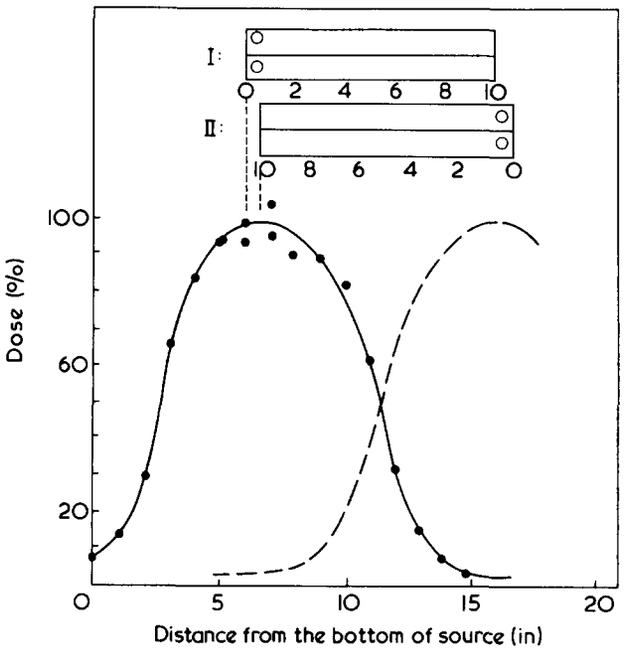

Figure 5 Geometric arrangement of parallel cleavage bars in ^{137}Cs source and resulting dose distribution

1/8 in. increments *versus* the 1/4 in. increments used previously[28]. The cases in which irradiation cracking necessitated the removal of a portion of a bar, unirradiated PMMA pinning blocks were carefully cemented into place to restore the original cleavage bar geometry (*Figure 4a*, upper). Some specimens were annealed for 24 h at 70°C.

Preparation of single edge notched tensile bar test specimens

Tensile bars were successfully prepared (*Figure 4b*) from material obtained by two techniques. In the first, tested cleavage bars were dissolved (≈75 g in 1–1.5 l) and shock precipitated (15 l) at sub-ambient temperatures (*Table 4*). From the percent recovery and the fact that the molecular weight distribution resulting from irradiation of PMMA could be described in terms of equation (10), the degree of polymerization below which the non-solvent fails to precipitate any additional molecules, x_t, was estimated[27,53]. The first three precipitations were consistent with data obtained by Fox *et al.*[52] in which a number of solvent/non-solvent combinations were used in the moderate molecular weight range (e.g. acetone/Skellysolve, in which $x_t \approx 50$). Similarly, the carbon tetrachloride/Skellysolve combination was adequate for the low molecular weight range ($x_t \approx 20$), although better but more hazardous systems exist. From these bars the effect of the hydrostatic pressure which results from the radiation-induced gaseous by-products, the effect of low molecular weight fractions on γ, and the independence of γ with test method were analysed.

The second technique involved the solution polymerization[54,55] of uninhibited methyl methacrylate (MMA) (Rohm and Haas Co., Philadelphia, Pa.) under nitrogen at 60°C. *Table 5* summarizes the polymerization ingredients necessary to obtain the $\bar{M}_n$ as calculated from ref 55. Referring to *Table 5*, the batches designated as 5000, 1500 I, and 1500 II were precipitated in 10:1 Skellysolve and recovered by filtering at 20°C. Batch 1500 III was precipitated in 10:1 Skellysolve at –60°C. After excess supernatant was siphoned off and discarded, the solid precipitate was filtered at 20°C (designated 1500 III-a). The remaining filtrate was vacuum dried to a powder at 40°C and combined with 15 g of 1500 III-a (designated 1500 III-b). The 1000 I polymer solution was vacuum distilled to a viscous residue. One half of the residue was cast directly into sheet form, while the remainder was dissolved in methanol, precipitated in H_2O, and recovered by filtration at 20°C. This methanol/H_2O combination did not produce a material useful for testing. Batch 1000 II was precipitated in 10:1 n-hexane and filtered at –60°C. The % recovery of the filtered polymers was determined after drying at 40°–60°C for several days.

Table 4 Schedule of notched tensile bars prepared by precipitation of irradiated parallel cleavage bars

Original cleavage bar specimen no.	Calculated $\bar{x}_n$*	Solvent/non solvent combination	% Recovery
18	71	Acetone at 22°C/absolute EtOH at –50°C	77
20	41	Acetone at 22°C/absolute EtOH at –50°C	59
1	22	Acetone at 22°C/absolute EtOH at –50°C	40
2	52	CCl_4 at 22°C/Skellysolve B† at –20°C	95

* Ref 27

† A petroleum distillate composed primarily of hexane (b.p. 67°–69°C), Skelly Oil Company, El Dorado, Kansas

Table 5 Recipes for the solution polymerization of low molecular weight PMMA

Batch designation	Desired $\bar{x}_n$	MMA (g)	Toluene (g)	% AIBN*	% Butanethiol*	% Recovery*
5000	50	60	140	1	2.7	49
1500 I, II, III	15	60	140	1	9.1	41, 43, 50
1000 I, II	10	60	140	1	13.6	–, 52

* Based on monomer

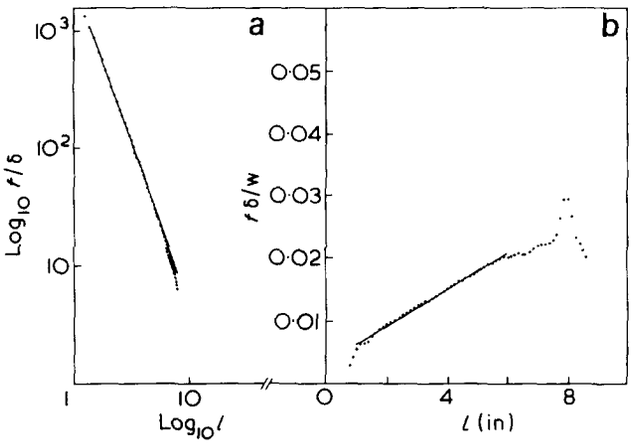

Figure 6 Data analysis of constant dose profile cleavage bar specimen no. 18 (see *Tables 3* and *7*): (a) determination of beam exponent (n) from the slope of $\log_{10} f/\delta$ *versus* $\log_{10} l$ plot, n = 2.67 (½ in width); (b) determination of γ from the slope of $f\delta/\omega$ *versus* l plot. γ = 298 erg/cm^2

Sheets of low molecular weight PMMA were made by placing the dry powders (or in the case of 1000 I, a heavy syrup) in an open tinfoil mould. After preheating the powder under a nitrogen atmosphere at temperatures that ranged from 120°–180°C, the powder was cast into a smooth sheet by repeated evacuation and nitrogen introduction. After annealing overnight under nitrogen at ~$0.9T_g$, the sheet was slowly cooled to room temperature. Only by utilizing a stress deformable foil and an extensive cooling scheme could such a brittle material be cast with reasonable success. After the usable portions of the 2–4 mm thick sheets were cut into strips using a diamond saw (Gillings–Hamco Thin Section Machine, Gillings–Hamco, Inc., Rochester, NY), a natural notch was introduced either by lightly applying pressure with a razor blade or with a specially fabricated wedge (based on an earlier design by Moskowitz; see *Figure 6* of ref 56). Last, the notched strip was mounted into two acrylic grips (*Figure 4b*).

Testing procedure

Both parallel cleavage and notched bars (i.e. stable *versus* unstable crack growth bars) were tested on an Instron machine (Instron Corp., Canton, Ma.) at crosshead extension rates of 6×10^{-5}–5×10^{-2} and 5×10^{-3}–1×10^{-1} cm/min, respectively. For the tensile bars, crosshead separation speeds were selected so that simple brittle fracture occurred (i.e. large specular zones with occasional river markings, small cleavage steps, or minute spalls) without introducing any 'gross' energy absorbing features (e.g. grainy textured surfaces and shards). Thereby, strain rates were limited to those values for which crack bifurcation phenomena were not a concern. Present work confirmed that such phenomena occurred whenever the release of stored elastic energy was greater than that which could be absorbed by increasing the crack velocity alone.

Data analyses

Cleavage bars were analysed according to the procedure delineated by Broutman and McGarry[23], utilizing the generalized beam formula:

$$f = a\delta l^n \tag{17}$$

where f is the applied force, δ is the deflection of one beam, l is the crack length from the pinning holes, and a and n are constants. By obtaining f *versus* δ' measurements ($\delta' = 2\delta + \Delta$, where Δ is the machine deflection), a plot of $\log f/\delta$ *versus* $\log l$ yields the slope n. By substitution of this value (which equals 2.67–3 for all molecular weights of PMMA tested) into the slope of an $f\delta/\omega$ *versus* l plot, γ is obtained:

$$f\delta/\omega = (4\gamma/n)l \tag{18}$$

where ω is the measured crack width. Because most of the cantilever bars prepared in the present work had constant dose profiles, the plots of $f\delta/\omega$ *versus* l obeyed a straight line relationship. Details on the treatment of a variable dose bar profile are given in ref 28.

Notched tensile bars were analysed using the equation of Srawley and Brown[57] for a plate of finite width:

$$\gamma = (f^2/2Et^2w)\,[7.59(c/w) - 32(c/w)^2 + 117(c/w)^3)] \tag{19}$$

To illustrate the influence of the free edge on the elastic strain energy field in close proximity to the crack tip, γ was also evaluated using the Griffith criterion for either plane stress (equation 20) or plane strain (equation 21) (ref 58);

$$\sigma_f = (2E\gamma/\pi c)^{1/2} \quad \text{for } c/w > 0.1 \tag{20}$$

or

$$\sigma_f = [2E\gamma/\pi c(1-\upsilon^2)]^{1/2} \quad \text{for } c/w < 0.1 \tag{21}$$

This comparison was particularly interesting for PMMA when $\gamma \lesssim 500$ erg/cm^2. In the present work a constant value for E (3.8×10^{10} dyne/cm^2) was used, as determined previously by three point bending down to $\bar{M}_n \approx 3 \times 10^3$ [27]. Likewise υ (0.32) was assumed constant.

Molecular weight determinations

In earlier work[4,27,28] molecular weights were computed from the known effects of radiation on the size of PMMA molecules[59,60] and confirmed by the limiting viscosity measurements from an equation of the form (see *Table 6*[61–64]).

$$[\eta] = K\bar{M}_v^{\alpha} \tag{22}$$

In the present work, the viscosity technique was used to calibrate the radiation source by serially sectioning an irradiated blank of PMMA (see *Figure 5*), while the molecular weights of irradiated specimens were calculated by an extrapolation of the observation that 100 eV of absorbed energy yields 1.7 chain scissions for doses $\lesssim$ 40 Mrad. Although the radiolysis of PMMA has now been extended to 500 Mrad[65], the initial limitations necessitated the substantiation of $\bar{M}_n$ by two adjunct techniques. The first method employed was vapour pressure osmometry, v.p.o. (Perkin–

Table 6 Viscosity–molecular weight relationships used for PMMA

Solvent	Temperature (°C)	$K \times 10^{+5}$ (dl/g)	α	$\bar{M}_v$ range $\times 10^{-4}$	Reference
Benzene	25	5.5	0.76	2–740	61, 62, 64
Benzene	30	195	0.41	0.3–2	63, 64

Table 7 γ results of cleavage bars tested (see *Table 3*)

Specimen No	Degassing period (days)	Tested dose profile (Mrad)	$\bar{x}_n$	Crosshead extension rate X 10^3 (cm/min)		γ (erg/cm^2)		Comments
3	136	105	36	5	3	213		a, e
4	186	105		5	2.67	242	190 ± 60	a, b
5	122	105		6, 0.6, 0.06	3	113		a, b
6	187	105		5	3	210		b
12	108	76 → 58	83	5	3	680		a, c
12	108	58 → 52	101	5	3	1000		a, c
8	142	95 → 69	54	5	2.67	497		a, b, c
13	111	76		5	3	483		a, f
14	46	76		1, 6	2.67	207		a, d, f
15	110	76		5	3	213	310 ± 130	b
16	64	79		5	2.67	121		a, b
17	64	79		5, 50	2.67	340		f
18	64	79		5	2.67	298		f
21	37	79		5	2.67	326		b
20	0	137	41	5	3	220		b, f

[a] Post-irradiation cracking
[b] Damaged part of bar cut-off and new pinning blocks attached
[c] Data reported as average $\bar{x}_n$ of tested dose profile
[d] Crosshead speed change during test
[e] Sinusoidal-like crack surface
[f] Canal-like crack surface

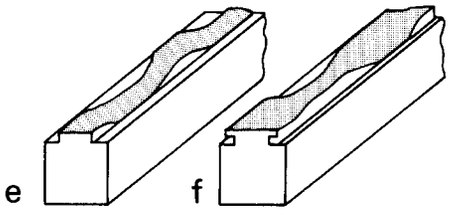

Table 8 γ results of notched tensile bars prepared by precipitation of irradiated parallel cleavage bars (see *Table 4*)

Original cleavage bar specimen no	$\bar{x}_n$	Crosshead extension rate X 10^2 (cm/min)	γ(erg/cm^2) Brown and Srawley	Griffith
18	85	1.0	970 ± 170 (7)*	770 ± 130 (7)
20	57	1.0	300 ± 80 (7)	250 ± 70 (7)
1	37	1.0	250 ± 130 (4)	200 ± 110 (4)
2	52	1.0	310 ± 90 (6)	250 ± 70 (6)

* Mean ± one standard deviation for the number of specimens tested in parentheses

Table 9 γ results of notched tensile bars prepared by solution polymerization (see *Table 5*)

Batch designation	$\bar{x}_n$	Crosshead extension rate X 10^2 (cm/min)	γ(erg/cm^2) Brown and Srawley	Griffith
5000	69	1.0	540 ± 220 (6)*	420 ± 160 (6)
1500 I	23	0.5	130 ± 100 (10)	100 ± 80 (10)
1500 II	25	1.0	150 ± 70 (3)	120 ± 50 (3)
1500 III-a	20	1.0	110 ± 10 (2)	70 ± 10 (4)
1500 III-b	16	1.0	170 ± 100 (3)	110 ± 70 (7)
1000 I	16	10	100 ± 60 (3)	70 ± 40 (4)
1000 II	16	10	100 ± 50 (8)	80 ± 40 (8)

* Mean ± one standard deviation for the number of specimens tested in parentheses

Elmer Model 115 Molecular Weight Apparatus, Perkin–Elmer Corp., Norwalk, Conn. and Wescan Model 233 Molecular Weight Apparatus, Wescan Instruments Inc., Santa Clara, Ca.), while the second method utilized differential thermal analyses (Dupont 990 Thermal Analyser, Dupont de Nemours, Wilmington, De.) and the depression of the T_g[65]. These methods were also used to determine the $\bar{M}_n$ of specimens prepared by chemical initiation.

RESULTS

When cleavage bars having a constant dose profile were fractured, data similar to that of *Figure 6* were generated. From such plots, two straight lines were formed: the first slope yielded the beam exponent (equation 17), while the second slope yielded γ (equation 18). For the present case of a 1/2 in. wide cleavage bar with a 1/3 wide slot per side that was annealed, cracked before irradiation, irradiated 79 Mrad, degassed 64 days, and tested at 5×10^{-3} cm/min, the total fracture surface energy equalled 300 erg/cm^2 and $n = 2.67$. Similar information was accumulated for each of 14 out of 21 cleavage bars that survived all procedures (*Table 7*). When compared with the preparation schedule of *Table 3*, these results showed that the slot type, annealed state, and precracked condition were, at most, of secondary importance. Moreover, within the range of values tested in *Table 7*, no effect on γ was noted from either varying the degassing period, the crosshead extension rate, or the mode of crack propagation (i.e. sinusoidal-like, canal-like or mixed – see inset). Since precise measurements are difficult on such brittle materials, similar doses were grouped together to obtain an accurate mean. The independent, overlapping data which follows show that the two tensile bar techniques support this premise.

The γ results of the notched tensile bars, which were prepared by precipitation of irradiated parallel cleavage bars and by solution polymerization, are presented in *Tables 8* and *9*. In *Table 8* four cleavage bars were recovered two of which had not been tested previously. As expected, comparison of *Tables 8* and *9* showed that the post-precipitation $\bar{x}_n$ was greater than the post-irradiation (i.e. calculated) $\bar{x}_n$ in three of the four cases. In the first three cases, the % recovery substantiated these relative differences, while in the fourth case the % recovery confirmed that the post-

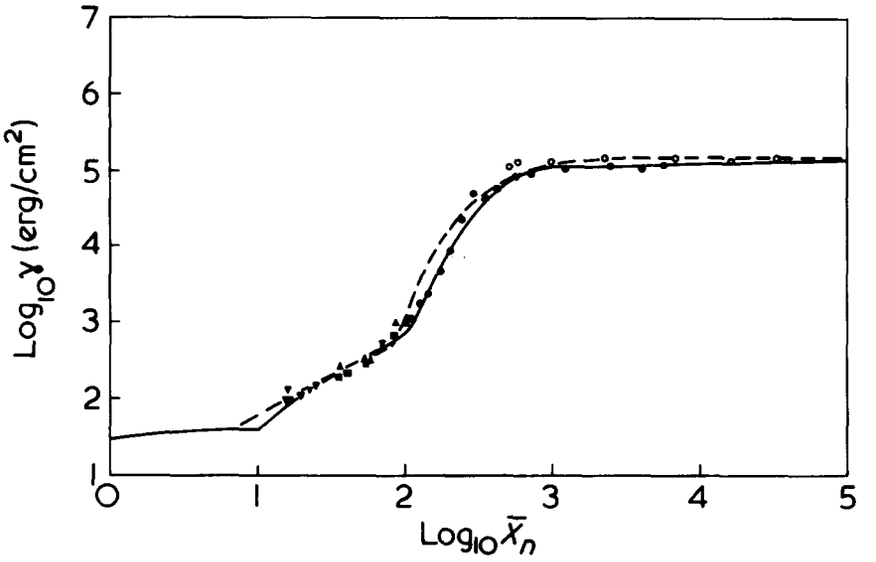

Figure 7 Comparison of PMMA fracture toughness data with model (——; see *Table 1* and text) and with computer analyses (— — —; see *Table 10*). Previous work: ○, cleavage bars prepared by chemical initiation (Berry[22]); ●, cleavage bars prepared by radiation degradation (Kusy and Katz[28]). Present work: ■, irradiated cleavage bars (*Table 7*); ▲, notched tensile bars prepared by precipitation of irradiated parallel cleavage bars (*Table 8*); ▲, notched tensile bars prepared by solution polymerization (*Table 9*). [Here, the notched tensile bar data was analysed by the Brown & Srawley criterion (equation 19)]

precipitation and post-irradiation $\bar{x}_n$ were equal. In addition to averaging both $\bar{x}_n$ and γ, γ was analysed according to the Brown and Srawley and the Griffith criteria.

Using the same format as *Table 8*, *Table 9* shows similar results for notched tensile bars prepared by solution polymerization. Comparison of *Table 9* with *Table 5* shows that a value of $\bar{x}_n < 16$ was unobtainable, independent of polymerization and recovery conditions. The reason for such behaviour was evident when the dried and filtered polymer was compared with a properly prepared vacuum cast sheet. For the 1000 series, a plasticization effect occurred, if sufficient time at temperature and partial nitrogen pressure were not allowed. Hence for the same solvent power the % recovery for the 5000 series was expected to be greater than the 1500 I and 1500 II series, while no advantage was gained either from the lower inherent $\bar{x}_n$ of the 1000 series or the reduced solvent power. Such a limitation supported the initial assumption that $(\bar{x}_n)_{L\to s} = 10$ (see *Table 1*) and emphasized the need to avoid any oligomers which would have a plasticizing effect on the physical properties.

The combined experimental results are shown in *Figures 7* and *8*. Here the mean data points, obtained either by cleavage bar (■, *Table 7*) or tensile bar fracture toughness tests (▲, *Table 8*; ▼, *Table 9*), are displayed with respect to the previous mean cleavage bar data points of Berry (○)[22] and Kusy and Katz (●)[28]. The two Figures thus generated show the results of the single edge notched data as calculated by Brown and Srawley (*Figure 7*) *versus* the Griffith criterion (*Figure 8*). In both Figures, the solid line represents the theoretical total fracture surface energy elucidated in equations (11)–(13).

DISCUSSION

Analysis of PMMA γ results

In general, the theoretical function and the experimental data of *Figures 7* and *8* correlated well, although the data points calculated by the Griffith criterion fit better (*Figure 8*). It is not known whether such a fine distinction was merely the result of a fortuitous selection of constants or whether the effect of the proximity of the free edge in very brittle materials has been overestimated. However, it is known that the results obtained via the Brown and Srawley criterion were, on average, 25% greater than those computed via the Griffith criterion.

A systematic examination of *Figures 7* and *8* reveals several interesting points. In the case of commercially useful products ($\bar{x}_n \gtrsim 10^3$), the fracture toughness is relatively constant[4,22,27,28], although the fatigue strength continues to improve[30]. Then as $\bar{x}_n$ decreases a decade, γ drops precipitously over two orders of magnitude thereby transforming PMMA from a ductile – i.e. a highly energy absorbing material – to a brittle material[4,27,28]. In the brittle region ($10 \lesssim$

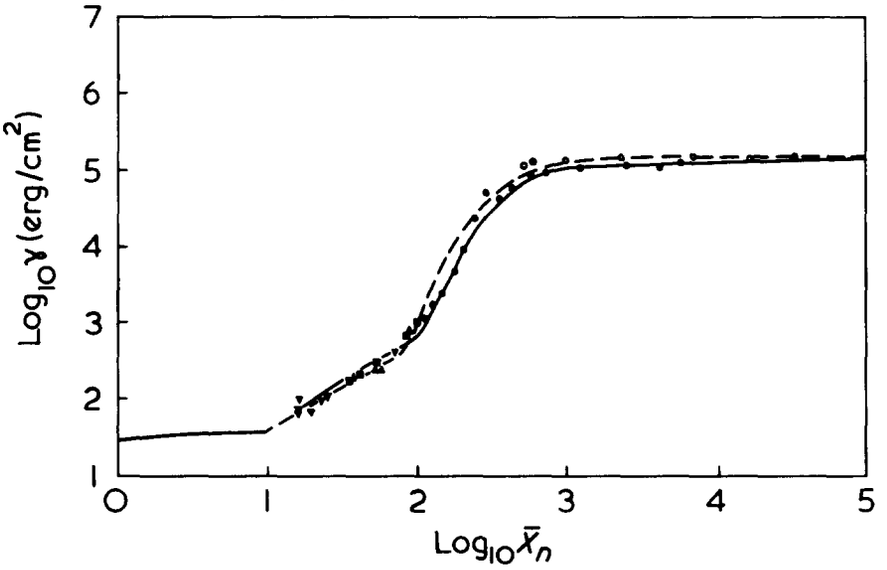

Figure 8 As *Figure 7* except that notched tensile bar data were analysed by the Griffith criterion (equations 20 and 21)

Table 10 Constants describing the total fracture surface energy as derived from non-standard linear regression analyses

Term	Poly(methyl methacrylate)		Polystyrene	
	Assigned value	Selected value*	Assigned value	Selected value
γ_∞	42.4 erg/cm^2		40.7 erg/cm^2	
k_e	290.8		236.6	
k_s	3.937		3.259	
γ_ϵ		250 erg/cm^2; 250 erg/cm^2		1 500 erg/cm^2
ϵ		46 ; 54		650
$(\bar{x}_n)_{L\to s}$		7 ; 10		1
x		730 ; 730		4 200
γ_c		150 000 erg/cm^2; 150 000 erg/cm^2		2 300 000 erg/cm^2

* First value was based on data evaluated via theory of Brown and Srawley. The second value was based on data evaluated using the Griffith criterion

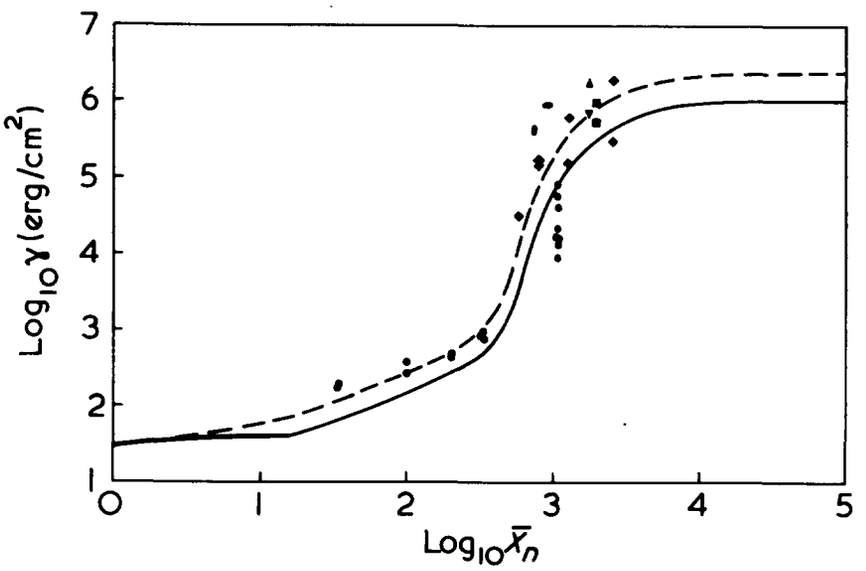

Figure 9 Comparison of polystyrene fracture toughness data with model (——; see *Table 2* and text) and with computer analyses (— — —; see *Table 10*). Symbols explained in Table below

Investigators	Test method	Comments	Ref
Benbow (◆)	Wedge splitting	Assumed $\bar{M}_w/\bar{M}_n \sim 2$	16
Berry (▼)	Cleavage	—	19
Berry (▲)	Tensile	Mean of ~ 100 values	17
Boogaart and Turner (■)	Tensile	Assumed $\bar{M}_w$ = 350 000–450 000 (source: Shell Co.)	21
Broutman and McGarry (●)	Cleavage	Assumed $\bar{M}_w$ = 190 000 ($\bar{M}_w/\bar{M}_n$ = 2.5) (Source: Dow Chemical Co.)	23
Robertson (●)	Cleavage	Sandwich of approximately monodispersed polystyrene (10 μm thick) and poly(methyl methacrylate)	29
Svennson (●)	Wedge splitting	$\bar{M}_w$ = 190 000	18

$\bar{x}_n \lesssim 10^2$), the variation of experimental conditions shows that γ is independent of material preparation (radiation *versus* chemical) and test bar geometry (tensile *versus* cleavage). The first observation substantiated earlier work which indicated that PMMA undergoes chain scission without significant crosslinking on exposure to ionizing radiation[60,65,66]. The second observation confirmed that γ, if tested at low crack velocities so that crack bifurcation was not a problem, was independent of test methodology[25]. As was observed previously[27], γ was not affected by the hydrostatic tensile stress that resulted from radiation-induced gas formation (see *Tables 7–9*, i.e. ● and ■ vs. the other samples). Similarly, no effect was noted by changing the molecular weight distribution (e.g. by the elimination of low molecular weight fractions – compare *Tables 8* and *7*), suggesting that the number-average was the controlling factor. Thus the present experimental data confirm the linear theoretical relationship proposed in equations (8a) and (12): when under stress, the entire molecule is the segment of interest that acts independently provided that no plasticization (i.e. $\bar{x}_n \nleq (\bar{x}_n)_{L\to s}$) or entanglement effects (i.e. $\bar{x}_n \ngeq \epsilon$) occur. Note that at the discontinuity, $\log_{10}\bar{x}_n = 1$, PMMA transforms from the solid glassy state first to the rubbery region then to the liquid flow region. In the latter region, any of the surface tension expressions (equations 7a, 7b, and 11) aptly describes the double solid line.

Although the theoretical solid line was intended to represent the most reliable results of the physical constants, the wide variation of reported values yielded a subjective choice. Consequently, a more objective data analysis method of using non-standard linear regression analyses was sought. By utilizing the general functional relationships and by floating five of the 'so-called' constants within broad boundaries, an optimum solution was generated for *Figures 7* and *8* (broken lines) from the selected values of *Table 10*. When *Table 10* was compared with *Table 1*, the constants were in general agreement. For the present purpose the distinction between tensile bar data, as analysed by the Brown and Srawley *versus* the Griffith criterion, was of secondary importance. Note, however, that recent inquiries have indicated that $(\bar{x}_n)_{L\to s} \approx 10$ (see ref 67).

Analysis of polystyrene γ results

Polystyrene is the only other polymer for which extensive studies of total fracture surface energy as a function of degree of polymerization have been attempted[16–19,21,23,29]. Using the same format as *Figures 7* and *8*, *Figure 9* was compiled from the literature underlying the Figure. This tabulated data shows much more scatter than the present PMMA; but

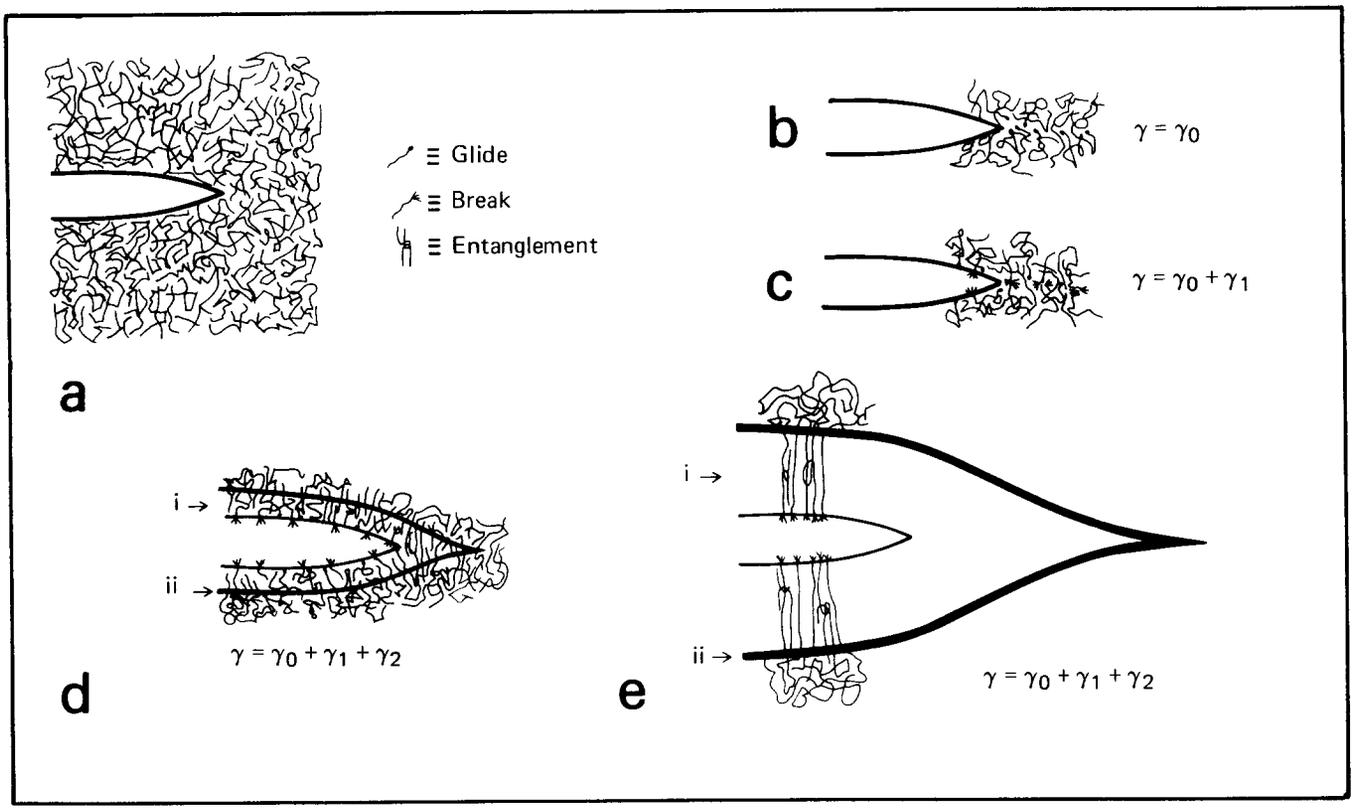

Figure 10 Schematic representation of molecular events which determine the fracture surface energy in a glassy polymer. (Derived, in part, from concepts presented by Berry[3,70], Dugdale[76] and Kambour *et al.*[31,51])

unlike PMMA, no discrimination was made between the tests that reflected fracture velocity effects and data that did not. When the theoretical expressions developed above were plotted, the full line was obtained. Qualitatively, the overall trend was encouraging, although the fit was marginal. Using the non-standard linear regression analyses approach, a better fit with the experimental data resulted. However, comparison of computer selected values (*Table 10*) with the most reliable literature values (*Table 2*) showed that $(\bar{x}_n)_{L\to s} = 1(?)$ *versus* $(\bar{x}_n)_{L\to s} = 15$. Information obtained from one manufacturer indicated that $T_g \approx 30°C$ when $(\bar{x}_n)_{L\to s} = 10$[68]. In a detailed study of the glass transition of polystyrene, Ueberreiter and Kanig found that $T_g \approx 19°C$ when $\bar{x}_n \approx 7$[69]. Based on an $\bar{x}_n \approx 7-10$ and the current theoretical expressions, the best solution lies between the two extremes.

Structure–property relationship

The present total fracture surface energy measurements provide a clearer understanding of the molecular activity that yields those values (*Figure 10*). When a tensile stress is applied to a suitably notched specimen (see *Figure 10a*), the total fracture surface energy measurement depends on three molecular events: the amount of sliding of one molecule past another (i.e. glide), the number of fractures of covalent bonds (i.e. breaks), and the extent of physical interpenetration of networks (i.e. entanglements). In a monomer, or other oligomers for which $\bar{x}_n \lesssim (\bar{x}_n)_{L\to s}$, simple failure occurs as the molecules glide away from the fracture plane (*Figure 10b*). In polyethylene the extent of that glide is termed a flow unit and represents 20–25 carbon atoms[72,73], or roughly $\bar{x}_n = 10$. (In the present work, such a flow unit corresponds to any $\bar{x}_n \lesssim (\bar{x}_n)_{L\to s}$!). As the solid state is attained ($\bar{x}_n > (\bar{x}_n)_{L\to s}$), chain mobility is sufficiently limited so that some covalent bonds rupture (*Figure 10c*). Here the glide component (γ_0) is supplemented by the break component (γ_1). Moreover, with each additional mer an equal increment of γ_1 is contributed until approximately one third of the bonds are broken. Beyond this juncture, physical entanglements occur as the molecules exceed some critical length. In response to the triaxial stress at the crack tip, the molecular alignment continues parallel to the applied tensile stress. When the molecular weight becomes great enough ($\bar{x}_n \approx x$), this transition zone (zone ii in *Figure 10d*) creates an organized network composed of aligned fibre bundles formed from the glide of entangled molecules, i.e. a craze (zone i in *Figure 10d*). With further molecular weight increments, γ_2 increases as the craze layer becomes much thicker (*Figure 10e*). Eventually, however, growth is increasingly opposed by more extensive molecular chain entanglements which are too interpenetrating for all to be incorporated into the craze. For PMMA this ultimately results in a limiting craze layer thickness of $12-14 \times 10^3$ Å and a transition zone of $2-10 \times 10^2$ Å [31,51] as $\gamma \approx \gamma_c$. Since defects must pile up in the transition zones, failure at these craze interfaces is not surprising[71,74,75]. Such constraints may be reduced only if time is allowed for disentanglements to occur, e.g. in fatigue[30].

Future work

The most pressing need is to obtain data on homologous series of other glassy, amorphous polymers. Polystyrene, therefore, is the logical first choice because the theory has been presented and the preliminary data gathered. Three other glassy polymers could be studied – poly(vinyl chloride), polycarbonate, and polysulphone – to supplement reported crack growth work[77]. In general, experimental procedures that would improve both the accuracy and the precision of γ measurements need further development[22,28,78].

CONCLUSIONS

From materials prepared by radiation degradation or chemical synthesis, the total fracture surface energy of PMMA was measured in the range $15 \lesssim \bar{x}_n \lesssim 100$. When these single edge notched tensile bar and cleavage bar results were combined with previous results, the influence of $\bar{x}_n$ on γ in the solid state was complete. These data provided the basis by which a model of the total fracture surface energy of PMMA was evaluated. From values abstracted from the literature, a similar comparison was made for polystyrene. Results showed that the model could predict γ by using the principle of superposition and several physical constants: γ_∞, γ_ϵ, ϵ, $(\bar{x}_n)_{L\to s}$, x, and γ_c. As an alternative approach, non-standard linear regression analyses provided another set of constants with which comparisons were made. The structure–property relationship was discussed at the molecular level in terms of chain glide, breaks, and entanglements. Future work should involve more accurate and precise γ measurements on other glassy polymers.

ACKNOWLEDGEMENTS

We thank Mr J. P. Price (American Enka Company) for the use of the vapour pressure osmometer, Mr L. Rosenblum (Wescan Instruments, Inc.) for determining x_n on specimens Nos. 1, 18 and 20 via v.p.o. (*Table 8*), and the UNC Physics Department for use of the ^{137}Cs source. Special thanks to Ms L. Lamson for her assistance in the computer analyses of the data and to Mr S. Adams (Rohm and Haas Company) for his suggestions regarding the solution polymerization procedures.

This investigation was supported by USPHS Research Grant No DE 02668 from the National Institute of Dental Research and, in part, by General Research Support Grant No RR 05333 from the General Research Support Branch of the National Institutes of Health. One of us (R.P.K.) also acknowledges support from Research Career Development Award No 1 KO4 DE 00052-02.

REFERENCES

1 Fox, R. B. and Zisman, W. A. *J. Colloid Sci.* 1950, **5**, 514
2 Advances in Chemistry Series No 43: 'Contact Angle, Wettability, and Adhesion' (Ed. R. F. Gould) American Chemical Society, Washington DC, 1964, p 11
3 Berry, J. P. *J. Polym. Sci.* 1961, **50**, 107
4 Kusy, R. P. and Turner, D. T. *Polymer* 1974, **15**, 394
5 Gallaugher, A. F. and Hibbert, H. *J. Am. Chem. Soc.* 1937, **59**, 2514
6 Fox, H. W., Taylor, P. W. and Zisman, W. A. *Ind. Eng. Chem.* 1947, **39**, 1401
7 Vogel, A. I. *J. Chem. Soc.* 1948, p 616
8 Jasper, J. J. and Kring, E. V. *J. Phys. Chem.* 1955, **59**, 1019
9 Roe, R. -J. *Proc. Nat. Acad. Sci. USA* 1966, **56**, 819
10 LeGrand, D. G. and Gaines Jr, G. L. *J. Colloid Interface Sci.* 1969, **31**, 162
11 Bender, G. W. and Gaines Jr, G. L. *Macromolecules* 1970, **3**, 128
12 Gaines Jr, G. L. *Polym. Eng. Sci.* 1972, **12**, 1
13 Wu, S. *J. Macromol. Sci. (C)* 1974, **10**, 1
14 Irwin, G. R. and Kies, J. A. *Welding J. Res. Suppl.* 1952, **31**, 95-S; *Ibid* 1954, **33**, 193-S
15 Benbow, J. J. and Roesler, F. C. *Proc. Phys. Soc. (B)* 1957, **70**, 201
16 Benbow, J. J. *Proc. Phys. Soc.* 1961, **78**, 970
17 Berry, J. P. *J. Polym. Sci.* 1961, **50**, 313
18 Svensson, N. L. *Proc. Phys. Soc.* 1961, **77**, 876
19 Berry, J. P. 'The Determination of Fracture Surface Energies by the Cleavage Technique' GEC Laboratory Report No 62-RL-(3034C), May 1962
20 Berry, J. P. *J. Polym. Sci.* 1963, **1**, 933
21 van den Boogaart, A. and Turner, C. E. *Trans. J. Plastics Inst.* 1963, **31**, 109
22 Berry, J. P. *J. Polym. Sci. (A)* 1964, **2**, 4069
23 Broutman, L. J. and McGarry, F. J. *J. Appl. Polym, Sci.* 1965, **9**, 589
24 Broutman, L. J. and McGarry, F. J. *J. Appl. Polym. Sci.* 1965, **9**, 609
25 Marshall, G. P., Culver, L. E. and Williams, J. G. *Plast. Polym.* 1969, **37**, 75
26 Green, A. K. and Pratt, P. L. *Eng. Fract. Mech.* 1974, **6**, 71
27 Kusy, R. P. and Turner, D. T. *Polymer* 1976, **17**, 161
28 Kusy, R. P. and Katz, M. J. *J. Mater. Sci.* 1976, **11**, 1475
29 Robertson, R. E. *Adv. Chem. Ser.* 1976, **154**, Ch 7
30 Kim, S. L., Skibo, M., Manson, J. A. and Hertzberg, R. W. *Polym. Eng. Sci.* 1977, **17**, 3
31 Kambour, R. P. and Barker Jr, R. E. *J. Polym. Sci.* 1966, **4**, 359
32 Williams, J. G., Radon, J. C. and Turner, C. E. *J. Polym. Eng. Sci.*, 1968, **1**, 30
33 Kusy, R. P. and Turner, D. T. *Polymer* 1977, **18**, 391
34 Zhurkov, S. N. and Abasov, S. A. *Vysokomol. Soedin.* 1961, **3**, 441
35 Rodriguez, F. 'Principles of Polymer Systems' McGraw–Hill, New York, 1970, Ch 7
36 Wu, S. *J. Colloid Interface Sci.* 1969, **31**, 153
37 Peebles, L. H. 'Molecular Weight Distributions in Polymers' Interscience, New York, 1971, Ch 1
38 Bovey, F. A. 'The Effects of Ionizing Radiation on Natural and Synthetic High Polymers', Interscience, New York, 1958
39 Wu, S. *J. Phys. Chem.* 1970, **74**, 632
40 Wu, S. *J. Polym. Sci.* 1971, **34**, 19
41 Wu, S. personal communication
42 Sudgen, S. *J. Chem. Soc.* 1924, **125**, 32
43 Quayle, O. R. *Chem. Rev.* 1953, **53**, 439
44 Roe, R. J. *J. Phys. Chem.* 1965, **69**, 1809
45 Zhurkov, S. N. *Int. J. Fract. Mech.* 1965, **1**, 311
46 Zhurkov, S. N., Regel, V. R. and Sanfirova, T. P. *Vysokomol. Soedin.* 1964, **6**, 1092 (translated in *Polym. Sci. USSR* 1964, **6**, 1201
47 Porter, R. S. and Johnson, J. F. *Chem. Rev.* 1966, **66**, 1
48 Bueche, F. 'Physical Properties of Polymers' Interscience, New York, 1962, Ch 3
49 Bueche, F. *J. Appl. Phys.* 1955, **26**, 738
50 Gubanov, A. I. and Chevychelov, A. D. *Fiz. Tverd. Tela* 1963, **5**, 91 (translated in *Sov. Phys. Solid State* 1963, **5**, 62
51 Kambour, R. P. *J. Polym. Sci.* 1966, **4**, 349
52 Fox, T. G., Kinsinger, J. B., Mason, H. F. and Schuele, E. M. *Polymer* 1962, **3**, 71
53 Valentine, L. *J. Polym. Sci.* 1955, **17**, 263
54 Sandler, S. R. and Karo, W. 'Polymer Synthesis – Vol. 1', Academic Press, New York, 1974, p 297
55 'Use of Acrylic Monomers in the Preparation of Low Number Average Molecular Weight Polymers' Rohm and Haas Technical Report TMM-23, March 1965
56 Moskowitz, H. D. and Turner, D. T. *J. Appl. Polym. Sci.* 1974, **18**, 143
57 Srawley, J. E. and Brown, W. F. NASA TND-2599 (1965)
58 Griffith, A. A. *Philos. Trans. Roy. Soc. (A)* 1921, **221**, 163
59 Charlesby, A. 'Atomic Radiation and Polymers' Pergamon, London, 1960, Ch 18
60 Kusy, R. P. and Turner, D. T. *J. Polym. Sci.* 1974, **12**, 2137
61 Schulz, G. V. and Meyerhoff, G. *Z. Elektrochem.* 1952, **56**, 904
62 Cantow, H. J. and Schulz, G. V. *Z. Phys. Chem.* 1954, **1**, 365
63 Fox, T. G., Mason, H. F. and Cohn, E. S. Rohm and Haas Report 19-146 and 24-62, July 27, 1959
64 Krause, S. Rohm and Haas Report 24-4, Feb 7, 1961
65 Kusy, R. P., Katz, M. J. and Turner, D. T. *Thermochim. Acta* in press

66 Shultz, A. R., Roth, P. I. and Rathmann, G. B. *J. Polym. Sci.* 1956, **22**, 495
67 Rohm and Haas Plastics Engineering Laboratory, personal communication
68 Baker, A. Dow Chemical Research Laboratory, personal communication
69 Ueberreiter, K. and Kanig, G. *Z. Naturforsch. (A)* 1951, **6**, 551
70 Berry, J. P. *J. Appl. Phys.* 1962, **33**, 1741
71 Friedrich, K. *Prakt. Metallogr.* 1975, **12**, 587
72 Roe, R. J. *J. Phys. Chem.* 1968, **72**, 2013
73 Kauzmann, W. and Eyring, H. *J. Am. Chem. Soc.* 1940, **62**, 3113
74 Doyle, M. J., Maranci, A., Orowan, E. and Stork, S. T. *Proc. Roy. Soc. London (A)* 1972, **329**, 137
75 Friedrich, K. *J. Mater. Sci.* 1977, **12**, 640
76 Dugdale, D. S. *J. Mech. Phys. Solids*, 1960, **8**, 100
77 Skibo, M. D., Hertzberg, R. W., Manson, J. A. and Kim, S. L. *J. Mater. Sci.* 1977, **12**, 531
78 Gilman, J. J. *J. Appl. Phys.* 1960, **31**, 2208